Practical Fin Shapes for Surface-Tension-Drained Condensation

M. A. Kedzierski
National Institute of Standards and Technology, Gaithersburg, MD 20899

R. L. Webb
The Pennsylvania State University, University Park, PA 16802

This paper introduces a new family of high-performance fin profiles for surface-tension-drained condensation. Previously described profiles for this situation have been defined in terms of the fin curvature and arc length. The existing profiles are generally not suitable for commercial manufacture. The fin profiles presented in this paper are conveniently defined by the fin tip radius, the fin height, and the fin base thickness. Consequently, the designer may easily specify a fin shape with parameters that are compatible with those used by the manufacturing industry. The heat transfer performance of the new profiles provides an improvement over existing, commercial fin shapes. An analysis is presented to show the R-11 condensation performance of the new profiles as a function of the geometric variables. A recommended design practice for fins for surface-tension-drained condensation is given also.

Introduction

This paper introduces a new family of high-performance fin profiles for surface-tension-drained condensation. It is intended that the new profiles be suitable for commercial manufacture. The focus of the paper is on the effect that the fin parameters have on the condensation heat transfer of the fin. The analysis presented here can be used to determine the best fin geometry for a given heat transfer surface. This analysis can also be used with the model of Webb et al. (1985), or the more recent model of Adamek and Webb (1989), to predict the condensation of a total tube.

Gregorig (1954) was the first to propose and design a fin profile that uses surface-tension drainage. Surface-tension forces are the dominant factor in determining the heat transfer for fins with fin heights less than 1.5 mm. The surface-tension enhancement is a result of a variation of the curvature of the liquid–vapor interface of the condensate film on the fin.

Figure 1 is an illustration of a vertical finned plate and the coordinate system used for the convex fin. A condensate film of thickness δ exists on the finned surface. The illustration shows the Gregorig fin profile having an arc length of S_m, and a drainage channel of depth L_s. The coordinate measured along the liquid–vapor interface is s. The coordinate measured along the fin surface is s'. The location $s' = 0$ is the point of symmetry of the fin arc and is referred to as the fin-tip. The angle θ measures the rotation of the liquid–vapor interface from the fin tip to an arbitrary point s. The condensate surface turns through a maximum angle of Θ_m, and a maximum arc length S_m.

Figure 1 shows that surface-tension forces drain the condensate film perpendicular to the direction of gravity (z direction) along the arc length S_m. Then, the condensate is carried by gravity in the channel. The pressure gradient (dP/ds) in the s direction due to surface-tension forces is given by

$$\frac{dP}{ds} = \sigma \frac{d\kappa}{ds} \tag{1}$$

where κ is the curvature of the liquid–vapor interface. Gregorig defined a shape for the convex profile, which would provide a constant film thickness over the entire arc length S_m. The required shape of the liquid–vapor interface is

$$\kappa = \frac{1.5\,\Theta_m}{S_m}\left[1 - \left(\frac{s}{S_m}\right)^2\right] \tag{2}$$

Adamek (1981) defined a family of convex shapes that use surface tension to drain the film. His fin curvature is defined as

$$\kappa = \frac{\Theta_m}{S_m}\left(\frac{\zeta+1}{\zeta}\right)\left[1 - \left(\frac{s}{S_m}\right)^{\zeta}\right] \text{ for } -1 \le \zeta \le \infty \tag{3}$$

where each value of ζ gives a fin profile with a different shape and aspect ratio (e/t_b). Figure 2 shows nine different Adamek profiles for ζ values within the range $-0.9 \le \zeta \le 30$. The profiles of the liquid–vapor interface, as shown in Fig. 2, start at $s = 0$ in the upper left corner and rotate through equal lengths of S_m.

Adamek used equation (3) along with equation (1) to cal-

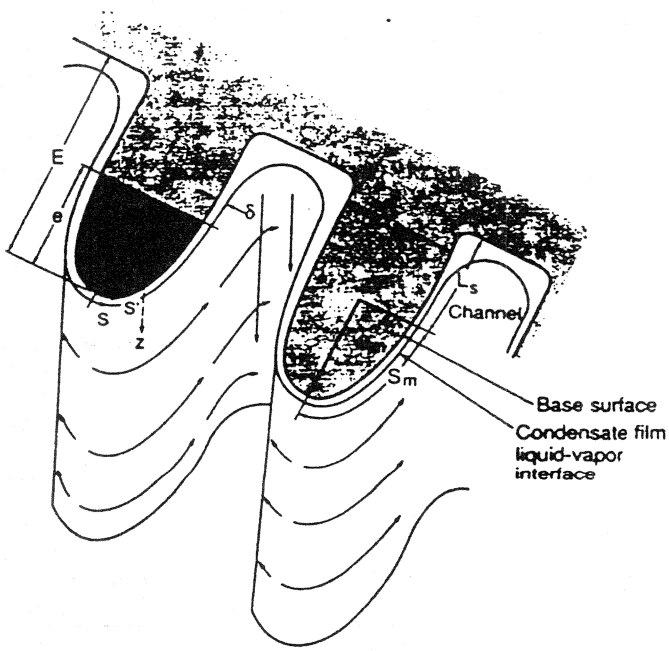

Fig. 1 Finned surface with film, streamlines, and coordinate system

Contributed by the Heat Transfer Division for publication in the JOURNAL OF HEAT TRANSFER. Manuscript received by the Heat Transfer Division December 23, 1988; revision received August 3, 1989. Keywords: Augmentation and Enhancement, Condensation, Finned Surfaces.

culate dP/ds, and paralleled Nusselt's analysis to solve the equation for the film thickness as a function of s ($\delta(s)$), i.e.,

$$\delta = \left(\frac{12\ B\ S_m^{\zeta+1} s^{2-\zeta}}{\Theta_m (\zeta+1)(\zeta+2)} \right)^{1/4} \tag{4}$$

where B is the property group $\nu k \Delta T_s/(\lambda\sigma)$. By integrating $1/\delta$ from equation (4) over $0 \le s \le S_m$, Adamek obtained the average condensate film thickness ($\bar{\delta}$), and using $\bar{h} = k/\bar{\delta}$ obtained the average heat transfer coefficient ($\bar{h}$)

$$\bar{h} = 2.149\ k \left(\frac{\Theta_m (\zeta+1)}{B\ S_m^3 (\zeta+2)^3} \right)^{1/4} \tag{5}$$

The Adamek profile for $\zeta = 2$ is identical to Gregorig's profile. If $\zeta = 1$ one obtains the results for dP/ds = const, a profile that was described by Zener and Lavi (1974).

"Practical" Fin Profiles

There are two primary applications for surface-tension-drained condensation. The first is for a vertical tube with axial fins, on which condensing may occur on the outer surface, and boiling occurs on the inner surface. Such service may be used in water desalination or gas liquefaction equipment. A second application involves horizontal, integral-fin tubes used in shell-and-tube heat exchangers.

Figure 3 shows the cross section of a fin from a commercially available integral-fin tube. The finned tube geometry is typically defined by specifying the tube diameter over the fins (D_o), the fins per meter (fpm), and the fin height (e). The fins of a commercially manufactured finned tube are formed by a thread rolling process. The rolling process uses a series of closely spaced "finning disks," to extrude the base metal from the tube wall into the narrow region between the finning disks. Figure 3 shows that the fins are of a trapezoidal shape, and that the sides are flat. Table 1 shows the dimensions of the fins, as reported by Webb et al. (1985). The fin thickness at the tip and the base are determined by the tooling requirements of the staged finning disks. This typically involves specification of a minimum desirable fin base and fin tip thicknesses, t_b and t_t, respectively. An extrusion process used to produce axial fins on vertical tubes also would establish the minimum desired fin base and tip thickness. Thus, the heat transfer designer typically specifies the D_o, fpm, and e dimensions, while the tooling engineer controls t_t and t_b and the fin shape.

The present analysis seeks to specify the fin shape and thickness dimensions to values that are acceptable to the tooling designer, and which provide favorable condensation performance. Thus, we seek to allow independent specification of the fin base thickness (t_b), the fin-tip radius (r_o), the fin height (e), and the angle Θ_m shown in Fig. 1. Unfortunately, the analyses of Gregorig (1954) and Adamek (1981) do not allow independent specification of e, t_b, r_o, and Θ_m. One may specify only S_m, Θ_m, and ζ. The values of ζ defines the fin aspect ratio, e/t_b. The value of e/t_b increases as ζ becomes smaller; see Fig. 2. This inability to specify e/t_b independently causes two practical problems. First, the Adamek $\zeta \le 1$ profiles all exhibit a zero fin-tip radius, which is physically impossible. Second, with fixed e, the fin thickness increases as ζ is increased ($\zeta > 0$). A large fin thickness will waste material and result in greater condensate retention than would exist with thinner fins. Hence, the Adamek family of fin profiles may not allow specification of the desired fin dimensions.

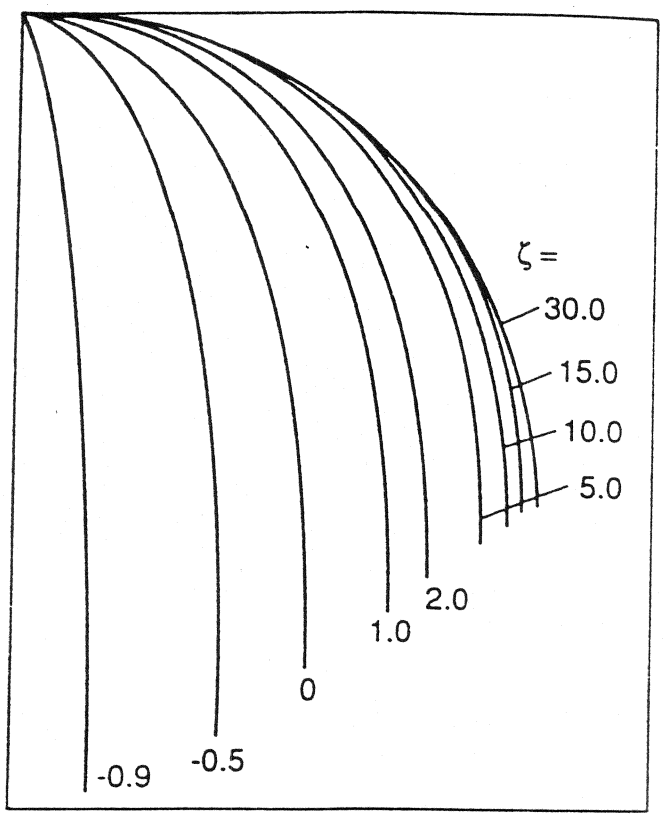

Fig. 2 Family of Adamek liquid-vapor interface profiles

Nomenclature

B = property group = $\nu k\ \Delta T_s/(\sigma\ \lambda)$, m
Bo = Bond number = $-\Delta\rho\ g/(dP/ds)$
D_o = tube diameter over fins, m
e = fin height of convex profile, m
E = total fin height = $e + L_s$, m
fpm = fins per meter, 1/m
g = gravitational acceleration = 9.806 m/s^2
h = heat transfer coefficient, W/(m^2 K)
k = thermal conductivity of condensate, W/(m K)
L_s = depth of drainage channel, m
P = pressure, Pa
r = radius of curvature of fin surface, m
r_o = radius of fin tip, m
S_m = total fin arc length, m
s = coordinate along liquid-vapor interface arc length, m
s' = fin arc length coordinate, m
T_s = saturation temperature of vapor, K
T_w = temperature of fin wall, K
t_b = fin thickness at base, m
t_t = fin thickness at tip, m
x = half fin thickness coordinate, m
y = fin height coordinate, m
z = coordinate perpendicular to x–y plane, m
Z = shape factor in new curvature equation
ΔT_s = $T_s - T_w$, K
$\Delta\rho$ = $\rho - \rho_v$, kg/m^3
δ = condensate film thickness, m
ζ = parameter in Adamek's curvature equation
θ = coordinate of fin, rad
Θ_m = maximum angle through which S_m turns, rad
κ = curvature of fin surface, 1/m
λ = latent heat of condensate, kJ/kg
μ = dynamic viscosity of condensate, kg/(m s)
ν = kinematic viscosity of condensate, m^2/s
ρ = density of condensate, kg/m^3
ρ_v = density of vapor, kg/m^3
σ = surface tension of condensate, N/m

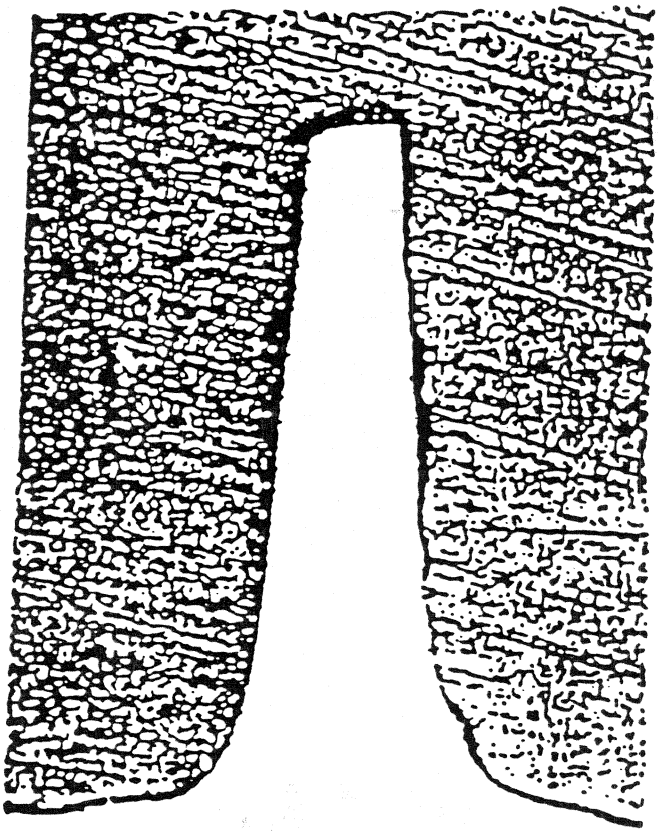

Fig. 3 Cross section of commercial 748-fpm integral fin

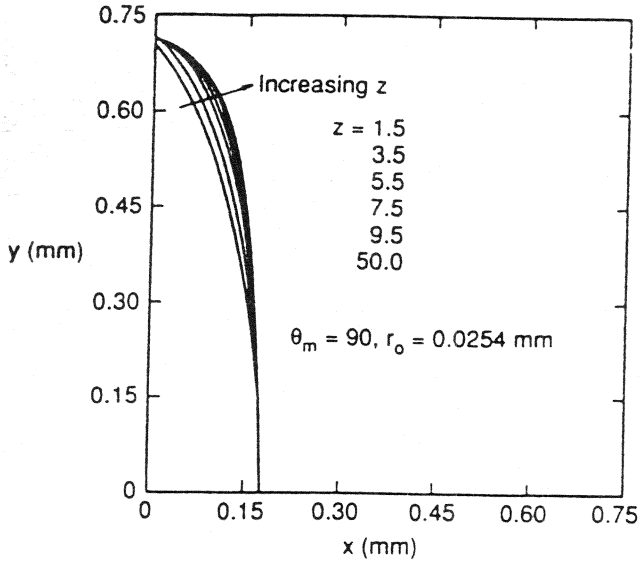

Fig. 4 Cross section of new profile for different values of Z

The new profiles described here allow specification of r_o and t_b independently of e and Θ_m. Analytical results are presented to show the effect of the several geometric parameters on condensation of R-11. These results are useful to determine the effect of manufacturing tolerances on condensation performance. One may use the analysis to select fin profiles that are manufacturable, and that provide high condensatoin performance. Guidance is provided for selection of the preferred geometric parameters.

Profile Definition

The new profiles, like the profiles of Gregorig and Adamek, are of the liquid–vapor interface. Since the condensate film is thin, the shape of the fin metal closely follows that of the liquid–vapor interface. Therefore, general observations concerning the liquid–vapor interface profile are valid for the solid–liquid profile also.

The new profile describes the fin shape in terms of t_b, r_o, e, Θ_m, and a shape factor parameter Z. The width of the fin tip can be reduced by lowering the value of Z; see Fig. 4. The Z is analogous to the ζ of Adamek that causes a variation in the aspect ratio of the profile. The equation to represent the profile was chosen such that the radius of curvature decreases for increasing θ. A linear combination of an exponential and a linear variation with θ permits an infinite range of functional forms depending on the magnitude of the multiplying constants. The radius of curvature (r) of the new profile is defined by

$$r = C_1 + C_2 \exp(Z\theta) + C_3\theta \tag{6}$$

The constants C_1, C_2, C_3 are given by

$$C_1 = r_o - C_2 \tag{7}$$

$$C_2 = \frac{0.5t_b(\sin\Theta_m - \Theta_m\cos\Theta_m) - e(\cos\Theta_m + \Theta_m\sin\Theta_m - 1)}{C_4 - (2(1-\cos\Theta_m) - \Theta_m\sin\Theta_m)} + \frac{r_o(\Theta_m\sin\Theta_m - 2(1-\cos\Theta_m))}{C_4 - (2(1-\cos\Theta_m) - \Theta_m\sin\Theta_m)} \tag{8}$$

$$C_3 = \frac{0.5t_b - C_1\sin\Theta_m - C_2 Z\exp(Z\Theta_m)\cos\Theta_m/(Z^2+1)}{\cos\Theta_m + \Theta_m\sin\Theta_m - 1} - \frac{C_2(\exp(Z\Theta_m)\sin\Theta_m - Z)/(Z^2+1)}{\cos\Theta_m + \Theta_m\sin\Theta_m - 1} \tag{9}$$

$$C_4 = (\exp(Z\Theta_m)(1-\cos\Theta_m + Z(\sin\Theta_m - \Theta_m)) + (Z\Theta_m - 1)\cos\Theta_m - (Z+\Theta_m)\sin\Theta_m + 1)/(Z^2+1) \tag{10}$$

The constants defined by equations (7)–(9) are obtained by applying the following boundary conditions to equation (6):

$$r = r_o \text{ at } \theta = 0 \tag{11}$$

$$t_b = 2\int_0^{\pi/2} r\cos\theta\, d\theta \tag{12}$$

$$e = \int_0^{\pi/2} r\sin\theta\, d\theta \tag{13}$$

The procedure to solve for the radius of curvature (r) of the new profile is outlined in the following. First, select e, t_b, Θ_m, r_o, and Z. Then evaluate C_4 given by equation (10) and substitute C_4 into equation (8) and solve for C_2. Next use C_2 to solve equation (7) for C_1. The constants C_1 and C_2 can now be used to solve for the remaining constant C_3.

Physically, it is convenient to define the fin in terms of x and y coordinates, where the y coordinate measures the fin height and the x coordinate measures half the fin thickness. Figure 4 shows a plot of six different fin cross sections plotted on x-y coordinates. The origin is at the center of the base of the fin. Equation (6) can be represented in rectangular coordinates (x, y) by integrating the x and y components of r, as done in equation (12) and equation (13). For example, the x coordinate can be obtained by changing the upper limit of integration of equation (12) from $\pi/2$ to θ, obtaining

$$x = \frac{C_2(Z\exp(Z\theta)\cos\theta + \exp(Z\theta)\sin\theta - Z)}{Z^2+1} + C_1\sin\theta + C_3(\cos\theta + \theta\sin\theta - 1) \tag{14}$$

The y coordinate can be obtained similarly by making the same

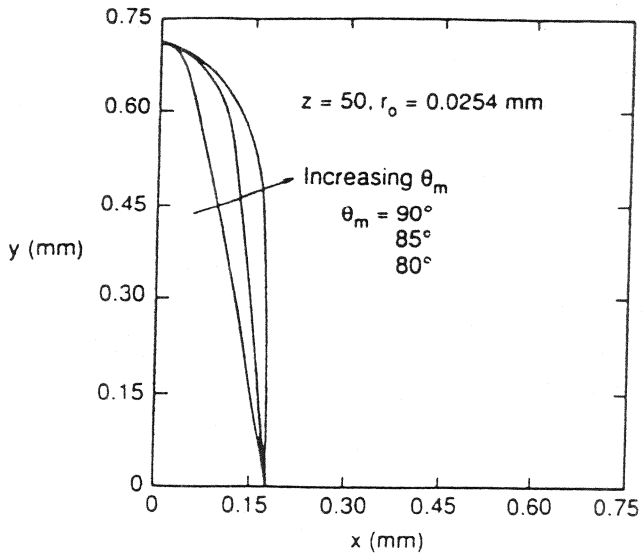

Fig. 5 Cross section of new profile for different values of θ_m

change to the upper limit of integration of equation (13). The result is

$$y = e - \frac{C_2(Z\exp(Z\theta)\sin\theta - \exp(Z\theta)\cos\theta + 1)}{Z^2+1} - C_1(1-\cos\theta) - C_3(\sin\theta - \theta\cos\theta) \quad (15)$$

The above procedure was used to evaluate the constants C_1 through C_4 along with equation (14) and equation (15) to determine the effect of Z and θ_m on the fin shape. Figure 4 shows the shape of the new profile for $t_b = e/2$, $r_o = 0.0254$ mm, and $\Theta_m = 90$ deg for various values of Z. The profile is shown to have wider fin tips for larger values of Z. Figure 5 shows the profile for $t_b = e/2$, $r_o = 0.0254$ mm, and $\Theta_m = 80$, 85, and 90 deg. Notice that a larger portion of the fin side is flat for the smaller Θ_m's.

Since the fin profile is a continuous function, one may proceed to develop an analytical solution for the condensation heat transfer coefficient (h), just as Adamek (1981) and Gregorig (1954) have done for their profiles. The key assumptions used to obtain equation (16) are: (1) laminar condensate flow; (2) surface tension in the s direction is the only driving force; (3) zero interfacial, vapor shear; and (4) constant fin temperature. The assumption that gravity forces are negligible compared to surface-tension forces can be checked by following the procedure given in the "Recommended Design Practice" section of this paper.

The film thickness of the new profile can be obtained by substituting the gradient of equation (6) with respect to θ ($dr/d\theta$) into the following:

$$\delta^4 = 4B\left[\frac{dr}{d\theta}\right]^{-4/3} r^4 \int_0^\theta \left[\frac{dr}{d\theta}\right]^{1/3} d\theta \quad (16)$$

Direct analytical integration of equation (16) proved difficult, so it was solved numerically. The discrete values of δ were used to calculate the average heat transfer coefficient from $h = k/[\int 1/\delta\, ds]/S_m$.

Kedzierski and Webb (1987) have experimentally verified the theories of Gregorig (1954) and Adamek (1981). Equation (16) was the basis of Gregorig's and Adamek's analyses. Therefore, a new theory with the curvature equation given here (equation (6)), substituted into equation (16), also is expected to predict the actual heat transfer. Consequently, no experimental data are given in this paper.

Table 1 Dimensions of fins on commercially available integral fin tubes with D_o = 19.0 mm

Fins/m	748	1024	1378
Fin height, e (mm)	1.53	1.53	0.89
Fin thickness at tip, t_t (mm)	0.20	0.20	0.20
Fin thickness at base, t_b (mm)	0.42	0.52	0.29
Aspect ratio, e/t_b	3.6	2.9	3.1

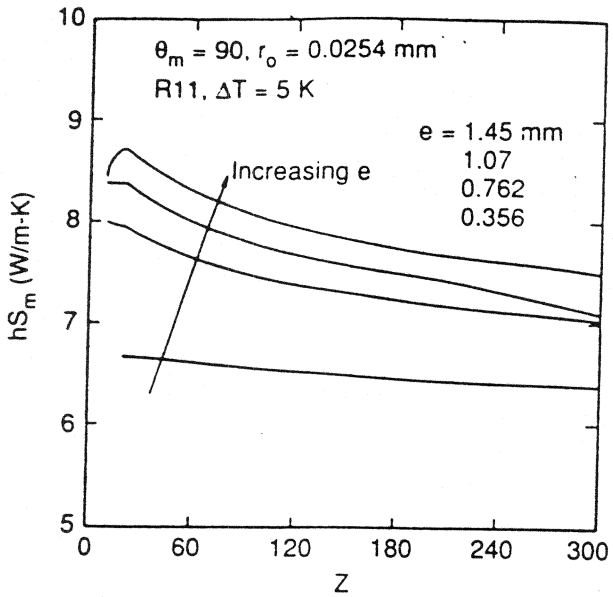

Fig. 6 Influence of Z on R-11 condensation at ΔT_s = 5 K

Condensation Performance of the New Profiles

R-11 condensation at 40°C with ΔT_s = 5 K was selected for illustration of the condensation performance of the new profiles. Four fins with the same t_b (t_b = 0.356 mm) but different fin heights (e = 0.356 mm, 0.762 mm, 1.067 mm, and 1.45 mm) were analyzed. These dimensions encompass the dimensional range of the commercial fin dimensions given in Table 1. The fin heights chosen are slightly lower than those of Table 1 to permit the addition of a 0.13-mm drainage channel, which makes the total fin height (E) compatible with those of Table 1. Thus, the total fin height is $e + L_t \equiv E$, as shown in Fig. 1. Heat transfer calculations for the above fins without drainage channels were done with variations on Z, r_o, and Θ_m to determine which parameters have the greatest influence on the heat transfer.

Figure 6 is a graph of the average overall heat conductance of the fin per unit fin length (hS_m) versus the shape factor (Z) for r_o = 0.0254 mm and Θ_m = 90 deg. Figure 6 demonstrates that the heat transfer is relatively insensitive to a wide range of Z. Recall from Fig. 4 that the shape factor represents the wideness of the fin tip. These results are encouraging since they demonstrate that for a given aspect ratio (e/t_b) a moderate deviation of the fin-tip shape will have little effect on the heat transfer of the fin. Thus, manufacturing tolerances associated with the shaping of the fin tip would tend to have a small effect on the heat transfer.

Figure 7 is a plot of hS_m versus the maximum angle through which the arc length turns (Θ_m) for r_o = 0.0254 mm and Z = 100. In general, Θ_m = 90 deg gives the highest heat transfer for all fin heights (aspect ratios). The Θ_m = 90 deg represents the maximum potential for the surface-tension pressure gradient for a given fin height. Angles less than 90 deg fail to use all of the available drainage force (curvature change) and consequently exhibit reduced heat transfer ability. For example, the hS_m of the e = 1.45 mm fin is reduced by 4 percent for

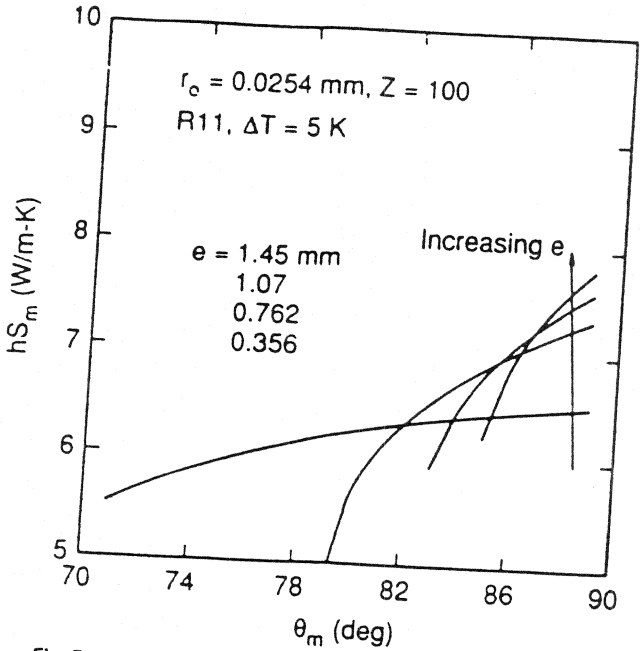

Fig. 7 Influence of θ_m on R-11 condensation at ΔT_s = 5 K

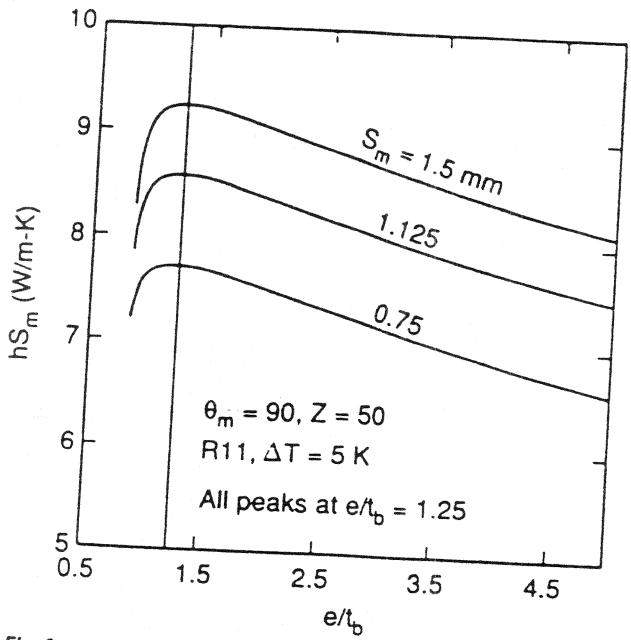

Fig. 9 Influence of aspect ratio and S_m on overall conductance

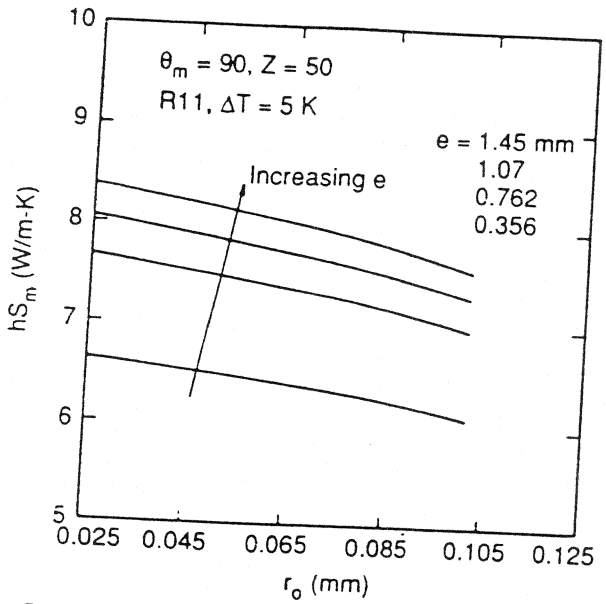

Fig. 8 Influence of r_o on R-11 condensation at ΔT_s = 5 K

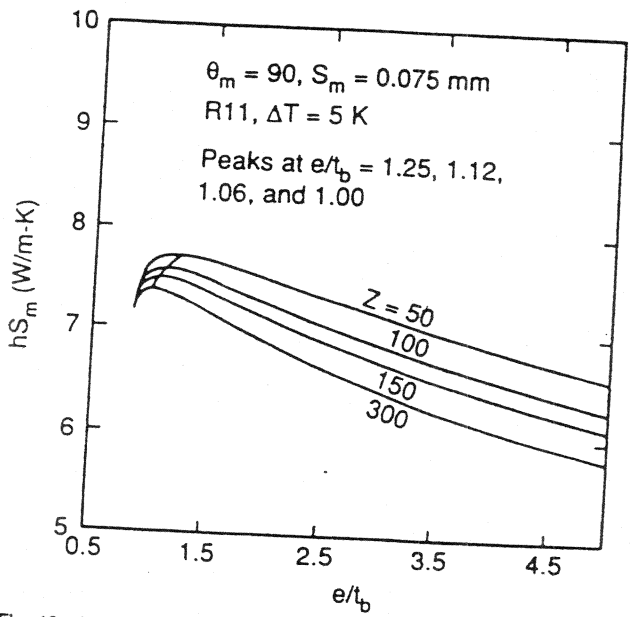

Fig. 10 Influence of aspect ratio and Z on overall conductance

each degree less than 90 deg. Also note that the heat transfer of the e = 0.762 mm fin for Θ_m = 79 deg is 37 percent less than that for Θ_m = 90 deg. Figure 7 demonstrates that the degradation of hS_m due to values of Θ_m less than 90 deg can be significant. Thus, the performance of the integral fin shown in Fig. 3 can be improved by increasing its Θ_m from 85 to 90 deg.

Figure 8 is a plot of hS_m versus the fin-tip radius (r_o) for Θ_m = 90 deg and Z = 50. Surprisingly, a 100 percent increase in r_o has a negligible effect on the heat transfer. As expected, the hS_m is larger for the smaller r_o, since this contributes to a higher average curvature for the fin. However, the above seems to support the observation that the fin-tip shape has a marginal effect on the heat transfer since r_o contributes to the shape of the fin tip.

Figure 9 is a plot of hS_m versus aspect ratio for the new fin geometry for R-11 with ΔT_s = 5 K, Z = 50, and different values of S_m. Figure 9 shows that the fins with larger S_m have higher heat transfer rates. There is a trade-off between increased surface area (S_m) and decrease in the magnitude of the average heat transfer coefficient (h) for higher fin heights. The reduction of h is due to a decrease in the surface-tension drainage force, which may become less than the gravity force if the fin height is too large. The hS_m rapidly decays for increasing e once the gravity force becomes dominant over surface tension. Guidance is given in a later section of this paper on how to determine the optimum value of e. Figure 9 also shows that the maximum hS_m for Z = 50 is at e/t_b = 1.25. The optimum aspect ratio is shown to be independent of S_m for fins of the same Z. The hS_m is shown to decrease by approximately 14 percent when the e/t_b is increased from 1.25 to 5.

Figure 10 illustrates the effect of e/t_b and Z on hS_m for a condensing length of 0.75 mm. The figure shows that for a given aspect ratio, fins with narrower fin tips (smaller Z) have larger hS_m values. For example, approximately a 10 percent

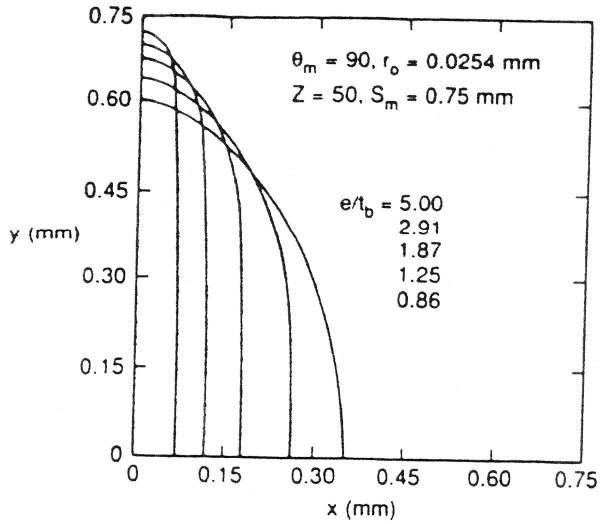

Fig. 11 Cross sections of new profile for different aspect ratios

increase in hS_m is achieved for a reduction of Z from 300 to 50. Consequently, the heat transfer of high-aspect-ratio ($e/t_b > 2$) fins can be increased slightly by reducing the width of the fin tip. Figure 10 also shows that for a given Z, the hS_m becomes smaller with increasing e/t_b for values of e/t_b greater than the optimum value. For example, the hS_m is shown to decrease by approximately 22 percent when e/t_b is increased from the optimum value to $e/t_b = 5$. The value of e/t_b that gives the optimum hS_m is larger for decreasing values of Z. For example, the optimum values of e/t_b for $Z = 50$, 100, 150, and 300 are 1.25, 1.12, 1.06, and 1.0, respectively. The Adamek profile $\zeta = -0.5$, which corresponds to $e/t_b = 2$, gives the optimum hS_m for his family of fins. The fin tip of the Adamek $\zeta = -0.5$ profile is narrower than the $Z = 50$ (narrowest Z). This is consistent with the above generalizations since the optimum e/t_b (2) for the $\zeta = -0.5$ profile (narrower fin tip) is larger than the optimum e/t_b (1.25) for the $Z = 50$ profile (wider fin tip).

Figure 11 shows the half cross section of the fins described by the uppermost curve of Fig. 10, i.e., for $Z = 50$, $r_o = 0.0254$ mm, $\theta_m = 90$ deg and $S_m = 0.75$ mm. Notice that for the same S_m the higher-aspect-ratio fins contain less fin material. Although the fin with $e/t_b = 1.25$ gives approximately 15 percent higher heat transfer than the $e/t_b = 5.0$ fin for the same arc length, it does so at the expense of three times the fin material. Also note that the t_b of the $e/t_b = 5.0$ fin is less than half that of the $e/t_b = 1.25$ fin. Consequently, at least twice as many of the high-aspect-ratio fins can be used per unit length on a tube than the lower aspect ratio fin. Although $e/t_b = 1.25$ gives the optimum h for a given S_m, a fin with a higher aspect ratio is more economical in terms of fin material and more energy efficient in terms of use with finned tubes.

It is important that the designer know the limitations of the fin parameters θ_m, r_o, and Z. The maximum value of θ_m is 90 deg for the fin shape given by equation (6). The smallest value of θ_m is set by the aspect ratio of the fin, i.e., θ_m (min) = arctan ($2e/t_b$). The smallest value of θ_m for a given aspect ratio corresponds to a fin of triangular shape. In order to have a fin of a particular e/t_b with a θ_m smaller than θ_m (min), the fin must be concave instead of convex. The largest r_o attempted in this analysis was 0.035 mm. The maximum r_o is directly proportional to S_m. For example, the r_o for a fin of constant radius is $r_o = S_m/\theta_m$. Consider this to be the upper limit of r_o. However, the maximum r_o for all fins will be less than S_m/θ_m since the radius of curvature decreases as the arc turns through θ_m. There were certain values of Z that caused the values of the exponential terms encountered in equation (6) to be outside the numerical range permitted by Fortran. Lower limits of Z were found to be around -0.01. Upper limits of Z were found to be around 500. The limitation of Z depends on the aspect ratio of the fin. For example, larger lower limits on Z are associated with larger aspect ratios. Hence, all fins will not necessarily fall within the above limits of Z.

Table 2 Comparison of hS_m on three profile types

Profile	Parameter	e (mm)	t_b (mm)	hS_m (W/m-s)
Gregorig	$\zeta = 2$	1.45	1.88	8.04
Gregorig	$\zeta = 2$	0.28	0.356	5.31
Adamek	$\zeta = -0.78$	1.45	0.356	9.45
New profile (r_o = 0.025 mm)	$Z = 10$	1.45	0.356	8.45

Comparison With Adamek and Gregorig Profiles

Table 2 compares the average h over the arc length (S_m) for $S_m = 1.485$ mm and $\theta_m = 90$ deg for all profiles. For a fin base thickness of $t_b = 0.356$ mm, the value of hS_m of the new profile is within 10 percent of the Adamek profile, which has a zero tip radius. The $r_o = 0$ profile Adamek is not practically attainable. Consequently, the calculated heat transfer coefficient for the Adamek profile is optimistically higher than what can be realistically achieved. However,the authors believe that if the Adamek profile had $r_o \neq 0$, the calculated heat transfer would be only 2–4 percent lower than that for $r_o = 0$. Thus, the actual difference between the heat transfer performance of the new profile and the Adamek profile for the same aspect ratio would be somewhat smaller than the calculated 10 percent.

Table 2 also shows that the $t_b = 0.356$ mm Gregorig profile has a small hS_m, because of its smaller fin height. If the fin height of the Gregorig fin is set at 1.45 mm, hS_m will increase, but the base thickness will be 1.88 mm. A 1.88-mm fin thickness will waste a considerable amount of fin material, and limit the fin density to considerably smaller values than for the $t_b = 0.356$ mm fins. The above discussion illustrates the disadvantage associated with the Gregorig fin by not being able to choose e and t_b independently.

Recommended Design Practice

The sensitivity investigation presented here can be used to provide some general guidelines for good fin design. It can be seen that fins with high aspect ratios result in high hS_m and large fpm, which implies high heat transfer per tube. Fins with $\theta_m = 90$ deg make better use of the surface-tension enhancement that fins with $\theta_m < 90$ deg. Therefore, it can be easily decided that the fin should always be designed for $\theta_m = 90$ deg. But how large can e be? And how small can t_b be?

Care must be taken to ensure that e is not so large that the surface-tension pressure gradient has dissipated over a significant portion of the fin. The Bond number (Bo), which is the ratio of gravity forces to surface-tension forces, can be used to test the strength of the surface-tension pressure gradient. If the surface-tension forces are dominant over gravity forces, then the condensate drainage is determined by surface-tension. The strength of the surface-tension pressure gradient weakens as the film approaches the base of the fin. The Bond number at the base of the fin can be approximated by

$$\text{Bo} = \frac{\Delta\rho\, g\, e^2}{\sigma\, \theta_m} \tag{17}$$

A Bo of 1 implies that surface-tension forces are equal to the gravity forces at the end of the fin and that surface-tension forces are greater than gravity forces for the remainder of the fin. Equation (17) should always be used to check first whether surface-tension forces are truly dominant (Bo < 1) over gravity

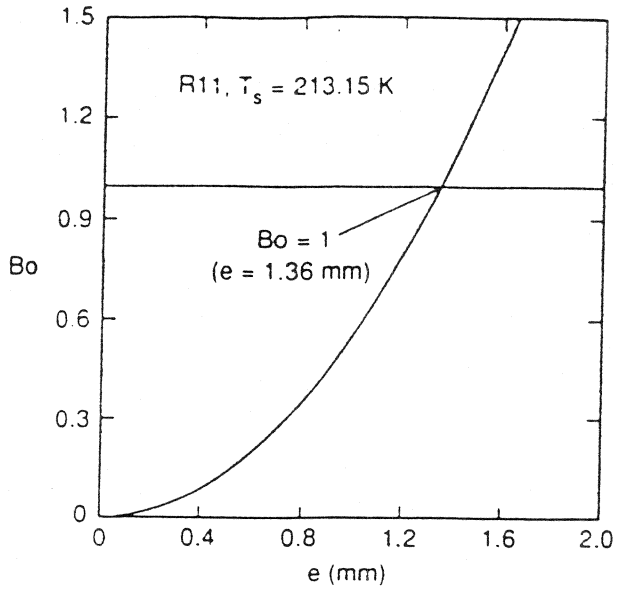

Fig. 12 Bond number as a function of e for R-11 at T_s = 213.15 K

forces before performing an analysis that assumes so. Notice that equation (17) predicts that small fin heights and large Θ_m give strong pressure gradients.

In order to achieve a high hS_m and maintain surface-tension drainage, the authors recommend that fin heights be designed to achieve Bo = 1. Figure 12 is a plot of equation (17) (Bo) for R-11 at T_s = 213.15 K versus e. The Bo becomes 1 at e = 1.36 mm. Consequently, a good fin height design is e = 1.36 mm for condensation of R-11 at T_s = 213.75 K. The Bo = 1 for this fin ensures that surface-tension forces are larger than gravity forces for the entire fin (with the exception of the very end of the fin). The advantage of a high fin height is in that a large hS_m is achieved. Fins larger than 1.36 mm will exhibit surface-tension drainage along the entire fin for higher surface-tension fluids, such as water.

Two other factors to consider when designing the fin height are tube-side pressure drop, and the condensation row effect. Small fin heights are beneficial for applications where low tube-side pressure drop is important. For a constraint on the overall diameter (D_o) of the tube, a large internal diameter is possible if the heights of the fins are small. However, Webb and Murawski (1988) have shown that high fin heights can benefit heat transfer by reducing the row effect caused by condensate inundation.

Two factors to consider when designing the fin thickness are condensate retention and the number of fins per meter. When condensed fluid is retained in the interfin spaces of the lower portion of a horizontal finned tube, the phenomenon is known as condensate retention. The condensed fluid acts as an insulating blanket on the tube. Consequently, severe degradation of heat transfer performance can occur with an increase in condensate retention. For a fixed fpm, one can reduce the condensate retention by reducing the fin thickness. Rudy et al. (1984) have investigated the trade-offs between increased heat transfer for larger fpm and the decrease in heat transfer for increased condensate retention for larger fpm. They have shown that an optimum fpm exists, for each fluid, which is a compromise between the two effects. In general, the optimum fpm is smaller for the higher surface-tension fluids. Also, the fin efficiency can be increased by reducing the fin thickness. Thus, a small t_b is one factor that can lead to finned tubes with high heat tranfser performance. The lower limit of t_b is dictated by the manufacturing process and the desired structural integrity of the fins.

Rudy et al. (1984) used the model of Webb et al. (1985) to predict the relationship between h and fpm for process-industry fluids. The Webb model uses the Adamek fin profiles in their prediction. An iteration for the Adamek fin with the proper aspect ratio is required in the calculation. The iterative procedure will be avoided if the new profiles presented here are used instead of the Adamek profiles in the analysis.

Conclusions

This work has defined fin profile shapes, which are practical for commercial manufacture. The designer may independently specify the fin-tip radius, the fin height, and the fin base thickness. The performance of the new profile with r_o = 0.025 mm is competitive with those of Gregorig and Adamek, for the same fin height. A sensitivity analysis of the parameters Z, r_o, S_m, and Θ_m on the performance of the new profile was presented. Fins with large S_m and Θ_m = 90 deg have large hS_m values. The hS_m decreases for decreasing values of Θ_m, and Θ_m = 90 deg always gives the optimum hS_m. For example, the hS_m of a fin with e = 1.45 mm is reduced by 4 percent for each degree less than 90 deg. The analysis shows that hS_m is moderately sensitive to Z (tip width). Fins with narrower fin tips have marginally higher hS_m values. For example, the heat transfer of high-aspect-ratio ($e/t_b > 2$) fins can be increased approximately 10 percent by reducing Z from 300 to 50. Also, the analysis has shown that a 100 percent increase in r_o has a negligible effect on hS_m. Consequently, the shape of the fin tip (r_o and tip wideness) does not need to be machined precisely. General design guidelines for selection of the geometric parameters are also given. The fin height and the fin thickness are more crucial design parameters than the shape of the fin. The authors suggest that fin heights be designed for Bo = 1 to ensure surface-tension drainage and large hS_m.

References

Adamek, T., 1981, "Bestimmung der Kondensationgroessen auf feingewellten Oberflaechen zur Auslegung optimaler Wandprofile," *Waerme- und Stoffuebertragung*, Vol. 15, pp. 255-270.

Adamek, T., and Webb, R., 1989, "Prediction of Film Condensation on Horizontal Integral-Fin Tubes," submitted to the *Int. J. Heat and Mass Transfer*.

Gregorig, R., 1954, "Hautkondensation an feingewellten Oberflaechen bei Beruecksichtigung der Oberflaechenspannunger," *Zeitschrift fuer angewandte Mathematik und Physik*, Vol. V, pp. 36-49.

Kedzierski, M. A., and Webb, R. L., 1987, "Experimental Measurements of Condensation on Vertical Plates With Enhanced Fins," *Boiling and Condensation in Heat Transfer Equipment*, ASME HTD-Vol. 85, pp. 87-95.

Rudy, T. M., Kedzierski, M. A., and Webb, R. L., 1984, "Investigation of Integral-Fin-Type Condenser Tubes for Process Industry Applications," *First U.K. Natl. Heat Transfer Conf.*, Vol. 86, pp. 633-647.

Webb, R. L., Rudy, T. M., and Kedzierski, M. A., 1985, "Prediction of the Condensation Coefficient on Horizontal Integral-Fin Tubes," ASME JOURNAL OF HEAT TRANSFER, Vol. 107, pp. 369-376.

Webb, R. L., and Murawski, C. G., 1988, "The Row Effect for R-11 Condensation on Enhanced Tubes," The Pennsylvania State University, unpublished.

Zener, C., and Lavi, A., 1974, "Drainage Systems for Condensation," ASME *Journal of Engineering for Power*, Vol. 96, pp. 209-215.